

Light Water Reactor Sustainability Program

BWR High-Fluence Material Project: Assessment of the Role of High-Fluence on the Efficiency of HWC Mitigation on SCC Crack Growth Rates

S. Teyssseyre

April 2014



The INL is a U.S. Department of Energy National Laboratory
operated by Battelle Energy Alliance



Light Water Reactor Sustainability Program

**BWR High-Fluence Material Project: Assessment of
the Role of High-Fluence on the Efficiency of HWC
Mitigation on SCC Crack Growth Rates**

S. Teyseyre

April 2014

**Idaho National Laboratory
Idaho Falls, Idaho 83415**

<http://www.inl.gov>

**Prepared for the
U.S. Department of Energy
Office of Nuclear Energy
Under DOE Idaho Operations Office
Contract DE-AC07-05ID14517**

DISCLAIMER

This information was prepared as an account of work sponsored by an agency of the U.S. Government. Neither the U.S. Government nor any agency thereof, nor any of their employees, makes any warranty, expressed or implied, or assumes any legal liability or responsibility for the accuracy, completeness, or usefulness, of any information, apparatus, product, or process disclosed, or represents that its use would not infringe privately owned rights. References herein to any specific commercial product, process, or service by trade name, trade mark, manufacturer, or otherwise, does not necessarily constitute or imply its endorsement, recommendation, or favoring by the U.S. Government or any agency thereof. The views and opinions of authors expressed herein do not necessarily state or reflect those of the U.S. Government or any agency thereof.

ABSTRACT

As nuclear power plants age, the increasing neutron fluence experienced by stainless steels components affects the materials resistance to stress corrosion cracking and fracture toughness. The purpose of this report is to identify any new issues that are expected to rise as boiling water reactor power plants reach the end of their initial life and to propose a path forward to study such issues. It has been identified that the efficiency of hydrogen water chemistry mitigation technology may decrease as fluence increases for high-stress intensity factors. This report summarizes the data available to support this hypothesis and describes a program plan to determine the efficiency of hydrogen water chemistry as a function of the stress intensity factor applied and fluence. This program plan includes acquisition of irradiated materials, generation of material via irradiation in a test reactor, and description of the test plan. This plan offers three approaches, each with an estimated timetable and budget.

CONTENTS

ABSTRACT.....	iii
ACRONYMS.....	viii
1. BACKGROUND.....	1
1.1 Review of Crack Growth Rate Data.....	1
1.2 Effect of Specimen Size on Stress Intensity Factor Validity and Irradiation Conditions	3
1.3 Data Required	6
2. PROGRAM PLANS.....	6
2.1 Program Plan Based on an Irradiation Program Dedicated to this Work.....	7
2.1.1 Material Selection	7
2.1.2 Specimen Design.....	7
2.1.3 Irradiation and Test Plan	7
2.1.4 Test Plan and Outcome	98
2.1.5 Estimate Cost	10
2.2 Program Based on Material Harvested from Boiling Water Reactor Components.....	10
2.2.1 Material and Specimens	11
2.2.2 Test Plan and Outcome	11
2.2.3 Estimated Timeline and Cost	12
2.2.4 Additional Irradiation Program and Test Plan	13
2.3 Programs Based on Materials Generated by a Previous Irradiation Program.....	13
2.3.1 Materials and Specimens	13
2.3.2 Test Plan and Outcome	14
2.3.3 Estimated Timeline and Cost	14
2.3.4 Extended Program.....	15
3. COLLABORATIONS AND BENEFIT TO OTHER FUNDAMENTAL PROGRAMS	16
4. REFERENCES	17

FIGURES

1. Effect of corrosion potential on the crack growth rate response of unsensitized 316 L, 20%CW	2
2. The NUREG-0313 disposition curve for stainless steels in normal water chemistry and hydrogen water chemistry.....	2
3. Crack growth rates as a function of stress intensity factor applied for doses greater than 3 dpa plotted against the Electric Power Research Institute disposition curve.....	3
4. Yield strength as a function of dose for stainless steels at 270 to 330°C according to [43]	4

5.	Temperature gradient obtained for a 0.5-CT specimen at the maximum flux rate considered in this report.....	6
6.	Schematic of the 0.4 T-CT specimen dimensions in inches	8
7.	Schematic of a tensile specimen dimension in inches	8

TABLES

Table 1.	Prediction of allowable stress intensity factor (ksi $\sqrt{\text{in}}$) for the specimen geometries considered for 304 stainless steel.	5
Table 2.	Prediction of allowable stress intensity factor (ksi $\sqrt{\text{in}}$) for the specimen geometries considered for 316 stainless steel (YS = 160 MPa).	5
Table 3.	Target dose for the irradiation program. The value in bold corresponds to the dose at which a capsule is removed and specimens are made available.	9
Table 4.	Test plan for 316L specimens.	10
Table 5.	Estimated timeline and associated cost for the irradiation program.	10
Table 6.	Control rod blade material available through collaboration.	11
Table 7.	Test plan for materials issued from harvested components.	12
Table 8.	Estimated timeline and cost assuming that the work is performed at Idaho National Laboratory for the basic test plan.	12
Table 9.	Estimated timetable for additional activity with control rod blade material.	13
Table 10.	Specimens available for the main program.	14
Table 11.	Specimens available for the extended program.	14
Table 12.	Stress intensity factor applied to HT304 specimens for the primary program.	14
Table 13.	Estimated timeline and cost for the primary program using specimen generated from a previous irradiation program.	15
Table 14.	Test plan for the extended program.	15
Table 15.	Estimated timeline and cost associated with the extended program.	16
Table A-1.	Example of test procedure.	19

ACRONYMS

ASTM	American Society of Testing and Materials
BWR	boiling water reactor
CGR	crack growth rate
CT	compact tension
EPRI	Electric Power Research Institute
HAZ	heat affected zone
HWC	hydrogen water chemistry
IASCC	irradiation- assisted stress corrosion cracking
JMTR	Japanese Material Test Reactor
K	stress intensity factor
NWC	normal water chemistry
SCC	stress corrosion cracking
CT	Compact Tension
TEM	Transmission Electron Microscope

BWR High-Fluence Material Project: Assessment of the Role of High-Fluence on the Efficiency of HWC Mitigation on SCC Crack Growth Rates

1. BACKGROUND

As power plants ages, it is necessary to determine if there are any changes in the behavior of the material as fluence increases and if the current disposition curves are sufficient to permit safe life extension of the reactors. In order to determine the remaining service life of the components, it is necessary to know the crack growth rate (CGR) of an existing flaw and to evaluate the allowable flaw size as fluence increases. For boiling water reactors (BWRs), locations like the core shroud experience 0.5 to 1×10^{20} n/cm² (about 0.14 dpa) per effective full power year at a flux around 2×10^{13} n/cm²-sec. This gives an accumulated fluence of $3\text{-}6 \times 10^{21}$ n/cm² (4-8.4 dpa) after 60 years of service and up to $4\text{-}8 \times 10^{21}$ n/cm² (5.6-11.2 dpa) after 80 years of service (Pathania et al. 2009). The few CGR data available at high fluence (i.e., greater than 3×10^{21} n/cm² or 4 dpa) suggest that the efficiency of the hydrogen water chemistry (HWC) mitigation technique decreases for the high stress intensity factor (K) applied. Although stress relaxation may sufficiently decrease K in service to minimize such an effect, there is concern that the disposition curve generated for lower fluence may not be conservative for high-fluence material. Moreover, a transition in the response of the material to irradiation-assisted stress corrosion cracking (IASCC) as a function of fluence suggests either a fundamental change in the cracking mechanisms involved or underlines the fact that the role of some local phenomena, peripheral with low dose material, becomes important as fluence increases. Therefore, it appears that confirming a change in the IASCC CGR response of a material as a function of K applied for increasing fluence level is not only valuable to assure safe operation of aging power plants, but it may be an opportunity to deepen our understanding of an IASCC mechanism that could have impact beyond the BWR community.

1.1 Review of Crack Growth Rate Data

HWC has been well established as an efficient mitigation technique for stress corrosion cracking (SCC) with unirradiated materials. CGR obtained in HWC can be 5 to 50 times lower than those obtained in normal water chemistry (NWC) (Andresen et al. 2002, Andresen and Morra 2008). Figure 1 shows the crack growth response when switching from an oxidizing environment (i.e., NWC) to a low potential environment (i.e., HWC) for a 316L stainless steel (20% cold work). In this case, the benefit of HWC is a decrease of CGR by 14. In the NRC-NUREG-0313 report (Hazelton and Koo 1988), the disposition curve for CGR as a function of K for unirradiated material is expressed as

$$\frac{da}{dt} = A \times K^{2.161} \quad (1)$$

where K is in Mpa \sqrt{m} and da/dt in m/s. With $A = 2.1 \times 10^{-13}$ in water containing 8 ppm DO and $A = 7.0 \times 10^{-14}$ in water with 0.2 ppm DO, which would correspond to low potential environment. In those curves (Figure 2), the HWC mitigation efficiency is credited with a factor of 3.

As a material accumulates dose, its susceptibility to SCC increases and cracking is said to occur by IASCC. CGR increases rapidly with dose and, compared to unirradiated stainless steels, it is common to find CGR elevated by a factor 5 or more for K greater than 10 Mpa \sqrt{m} . The Electric Power Research Institute (EPRI) proposed a CGR versus K disposition curve based on CGR data generated with material at fluence below 3×10^{21} n/cm² tested in BWR water chemistry conditions (Pathania et al. 2009). It is expressed as

$$\frac{da}{dt} = B \times K^{2.5} \quad (2)$$

where K is in Mpa \sqrt{m} and da/dt in m/s. $B = 4.564 \times 10^{-13}$ in NWC and $B = 1.51 \times 10^{-13}$ in HWC.

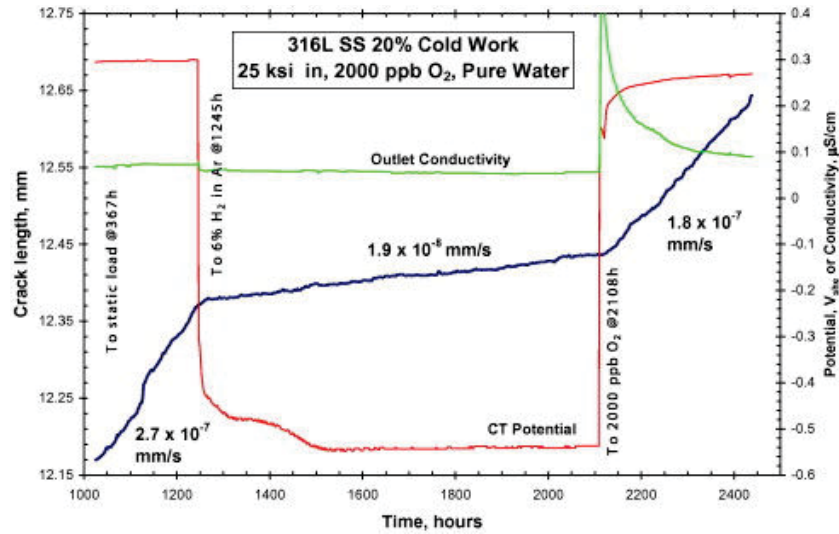


Figure 1. Effect of corrosion potential on the crack growth rate response of unsensitized 316 L, 20% Cold worked (from Andresen and Morra 2008).

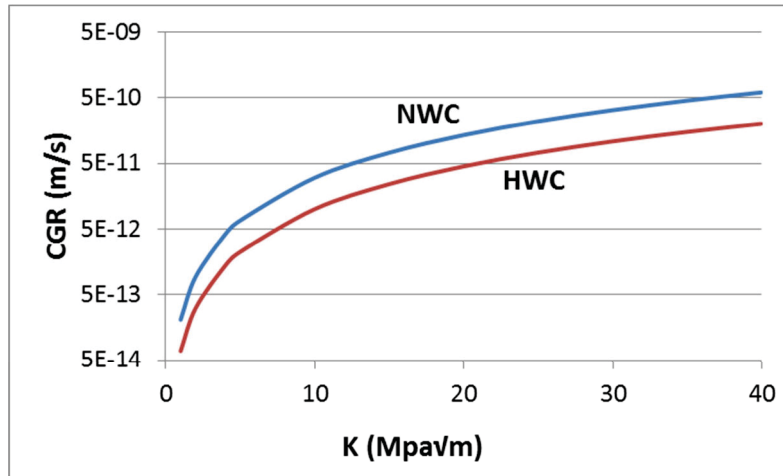


Figure 2. The NUREG-0313 disposition curve for stainless steels in normal water chemistry and hydrogen water chemistry.

When looking into the behavior of stainless steels irradiated above $3 \times 10^{21} \text{ n/cm}^2$, data suggest that the expected decrease in CGR when applying HWC may disappear as dose increases. Jensen et al. (2003) tested a control blade material that was in operation for about 23 years. The material accumulated about 12 dpa and was tested to a K up to 18 $\text{Mpa}\sqrt{\text{m}}$. They observed a high CGR in HWC and concluded that under such testing conditions, HWC did not mitigate IASCC. However, while testing a 304L core shroud material irradiated in the BOR-60 fast reactor at 5.5 and 10.2 dpa, Jensen et al. (2003) did observe lower CGR when testing at low corrosion potential; however, they did not see any K dependency between $K = 11 \text{ Mpa}\sqrt{\text{m}}$ and $K = 18 \text{ Mpa}\sqrt{\text{m}}$ (Jensen et al. 2009). Takamura et al. (2009) measured CGR for 316L and 304L tested in a BWR environment. They looked at the effect of Electro chemical corrosion potential (ECP) as fluence increases on CGR. Their findings suggest that the effect of ECP on CGR becomes weak when the K that is applied is greater than 20 $\text{Mpa}\sqrt{\text{m}}$. Horn et al. (2013) demonstrated that HWC did not decrease CGR when testing 316NG at 3 and 4 dpa under K greater than 18.7 $\text{ksi}\sqrt{\text{in}}$, although there was a noticeable decrease in CGR when a 4.6 dpa 316NG was tested at $K = 15.5 \text{ ksi}\sqrt{\text{in}}$. The IASCC growth rate of various grades of stainless steels materials tested in HWC and irradiated in BWR conditions are

plotted in Figure 3, along with the EPRI disposition curve for irradiated stainless steels in HWC. For K value greater than 15 ksi $\sqrt{\text{in}}$ (16.5 MPa $\sqrt{\text{m}}$), the CGR obtained are significantly above the disposition curves.

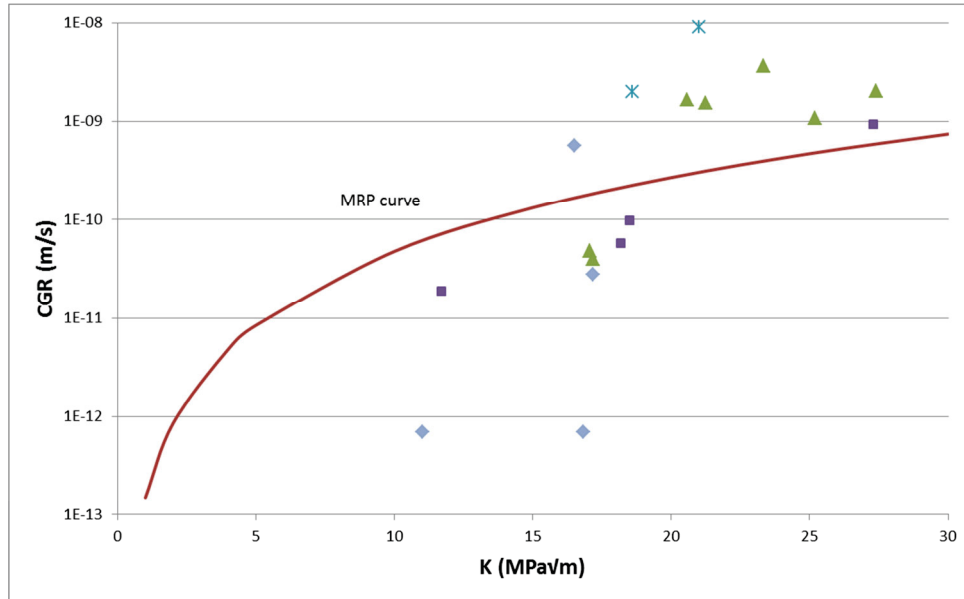


Figure 3. Crack growth rates as a function of stress intensity factor applied for doses greater than 3 dpa plotted against the Electric Power Research Institute disposition curve. The data used in this graph were extracted from (Jensen et al. 2003, Takakura et al. 2009, and Horn et al. 2013).

It is often mentioned that as fluence is accumulated in the material, radiation-induced stress relaxation occurs. As stress relaxes, the K experienced by the component will decrease and, therefore, high K may never be experienced by the component. Although stress relaxation occurs, it is nevertheless necessary to determine the evolution of CGR as fluence and K increases. Practically, such data can be used in correlation with stress relaxation data and weld residual stress prediction.

1.2 Effect of Specimen Size on Stress Intensity Factor Validity and Irradiation Conditions

The specimen size and mechanical properties determine the allowable K for each CGR testing. To prevent issues that would lead to invalid CGR data, the specimen should be designed to allow maintenance of K-size validity, while permitting application of the range of K selected and provision of sufficient material for crack advance during the various test segments. The stress intensity validity of a specimen is determined by the American Society of Testing and Materials (ASTM) E399 criteria (designed for plane strain fracture toughness testing) or ASTM E647 (designed for fatigue crack growth testing), which is less stringent. ASTM E399 is considered more appropriate for testing SCC. This standard provides the relationships between the geometry of the specimen and the mechanical properties of the material to determine the allowable K. The standard has been developed for material that exhibits work hardening. However, for irradiated materials that exhibit high yield stress (YS) due to radiation hardening and strain softening, the standard is not conservative. For irradiated materials, using an effective YS to determine K validity was proposed (Andresen 2011). The effective YS is defined as

$$YS_{eff} = \frac{YS_{irrad} - YS_{unirrad}}{\alpha} + YS_{unirrad} \quad (3)$$

where YS_{irrad} is the irradiated YS at temperature, $YS_{unirrad}$ is the unirradiated YS at temperature, and α is a discounting factor equal to 2 or 3 (based on experience).

YSeff is used in the following equations to determine the maximum K allowable at the beginning of the test and crack advance:

$$B_{eff} \geq 2.5 \left(\frac{K}{Y_{Seff}} \right)^2 \quad (4)$$

$$W - a \geq 2.5 \left(\frac{K}{Y_{Seff}} \right)^2 \quad (5)$$

where W is the width of the specimen, a the crack length, and B_{eff} the effective thickness as defined in Figure 4.

As fluence increases, irradiation hardening occurs, leading to an increase of YS. Figure 4 presents an estimation of the evolution of YS for 304 stainless steel and 316 stainless steel. These correlations have been developed by EPRI (Demma 2010). The YS_{irrad} predicted by these correlations has been used to calculate allowable K for several specimen geometries considered in this program. The results are summarized in Tables 1 and 2. When the allowable K decreases significantly as crack grow (a/w increase), the values at several a/w are given. Five compact tension (CT) specimen designs are considered: (1) standard 0.4 T-CT with normal thickness, (2) 0.4 T-CT with reduced thickness, (3) 0.5 T-CT with normal thickness, (4) 0.5 T-CT with reduced thickness, and (5) 0.6 T-CT with reduced length.

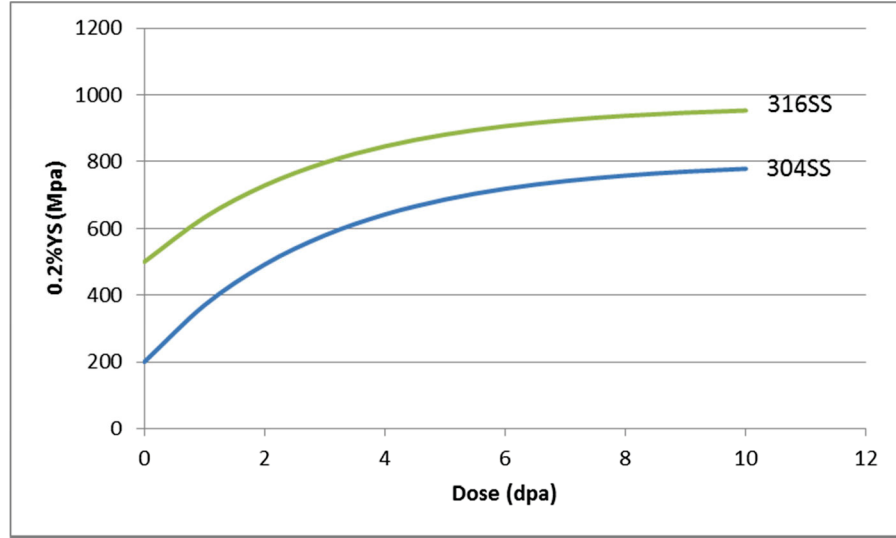


Figure 4. Yield strength as a function of dose for stainless steels at 270 to 330°C according to (Demma 2010)

It should be noted that the Nakamura et al. (2007) and Sumiya et al. (2007) analyses suggest that a stable, valid, CGR can be obtained even after K exceeds the upper limit determined with the effective stress concept. It also is accepted that the best determination of the validity of a CGR test is based on the cracking behavior recorded. However, considering that this report suggests the machining of specimens prior to irradiation, it is recommended to have a conservative approach when designing specimen.

In addition to influencing the maximum allowable K, specimen thickness also affects the temperature gradient across the specimen during irradiation. Figure 5 presents the temperature gradient obtained when a stainless steel 0.5 T-CT is being irradiated in the Advanced Test Reactor's pressurized water loop and receiving 1.58×10^{14} n/cm²-s (the highest flux rate considered in this report). The temperature difference between the specimen surface and the center of the specimen is 55°C (Tyler 2014). The temperature difference dropped to 35°C for a 0.4 T-CT specimen and is below 20°C for a specimen with a thickness

equal at 0.3 in. Therefore, using the thin specimen is encouraged when possible. Thin specimens also are advantageous because more can be irradiated in a test capsule.

Table 1. Prediction of allowable stress intensity factor ($\text{ksi}\sqrt{\text{in}}$) for the specimen geometries considered for 304 stainless steel.

Specimen Description	B_{eff}	W	2 dpa	4 dpa	8 dpa
Estimated Irradiated YS			491 Mpa	641 Mpa	758 Mpa
0.4 T-CT	0.38	0.8	$K_{\text{max}} = 18.4$	$K_{\text{max}} = 22.6$	$K_{\text{max}} = 25.9$
			$K_{\text{max}} (a/w:0.58) = 17.35$	$K_{\text{max}} (a/w:0.58) = 21.3$	$K_{\text{max}} (a/w:0.58) = 24.4$
					$K_{\text{max}} (a/w:0.65) = 22.3$
0.5 T-CT-1	0.28	0.8	$K_{\text{max}} = 15.8$	$K_{\text{max}} = 19.4$	$K_{\text{max}} = 22.3$
			$K_{\text{max}} = 20.4$	$K_{\text{max}} = 25.2$	$K_{\text{max}} = 28.8$
			$K_{\text{max}} (a/w:0.58) = 19.3$	$K_{\text{max}} (a/w:0.58) = 23.8$	$K_{\text{max}} (a/w:0.58) = 27.3$
0.6 T-CT	0.47	1	$K_{\text{max}} (a/w:0.65) = 17.6$	$K_{\text{max}} (a/w:0.65) = 21.7$	$K_{\text{max}} (a/w:0.65) = 24.9$
			$K_{\text{max}} = 15.8$	$K_{\text{max}} = 19.4$	$K_{\text{max}} = 22.3$
			$K_{\text{max}} = 22.5$	$K_{\text{max}} = 27.7$	$K_{\text{max}} = 31.8$
	0.57	1.2		$K_{\text{max}} (a/w:0.58) = 26.1$	$K_{\text{max}} (a/w:0.58) = 29.9$
			$K_{\text{max}} (a/w:0.58) = 21.2$	$K_{\text{max}} (a/w:0.65) = 23.8$	$K_{\text{max}} (a/w:0.65) = 27.3$

Table 2. Prediction of allowable stress intensity factor ($\text{ksi}\sqrt{\text{in}}$) for the specimen geometries considered for 316 stainless steel (YS = 160 MPa).

	B_{eff}	W	2 dpa	4 dpa	8 dpa
Estimated Irradiated YS			728 Mpa	846 Mpa	937 Mpa
0.4 T-CT	0.38	0.8	$K_{\text{max}} = 25.1$	$K_{\text{max}} = 28.4$	$K_{\text{max}} = 31.0$
			$K_{\text{max}} (a/w:0.5) = 25.75$	$K_{\text{max}} (a/w:0.58) = 26.7$	$K_{\text{max}} (a/w:0.58) = 29.1$
			$K_{\text{max}} (a/w:0.58) = 23.6$	$K_{\text{max}} (a/w:0.65) = 24.4$	$K_{\text{max}} (a/w:0.65) = 26.6$
	0.28	0.8	$K_{\text{max}} = 21.5$	$K_{\text{max}} = 24.4$	$K_{\text{max}} = 26.6$
				$K_{\text{max}} (a/w:0.65) = 24.4$	$K_{\text{max}} (a/w:0.65) = 26.6$
0.5 T-CT-1	0.47	1	$K_{\text{max}} = 27.9$	$K_{\text{max}} = 31.6$	$K_{\text{max}} = 34.5$
			$K_{\text{max}} (a/w:0.58) = 26.4$	$K_{\text{max}} (a/w:0.58) = 29.9$	$K_{\text{max}} (a/w:0.58) = 32.6$
				$K_{\text{max}} (a/w:0.65) = 27.29$	$K_{\text{max}} (a/w:0.65) = 29.7$
	0.28	0.8	$K_{\text{max}} = 21.5$	$K_{\text{max}} = 24.4$	$K_{\text{max}} = 26.6$

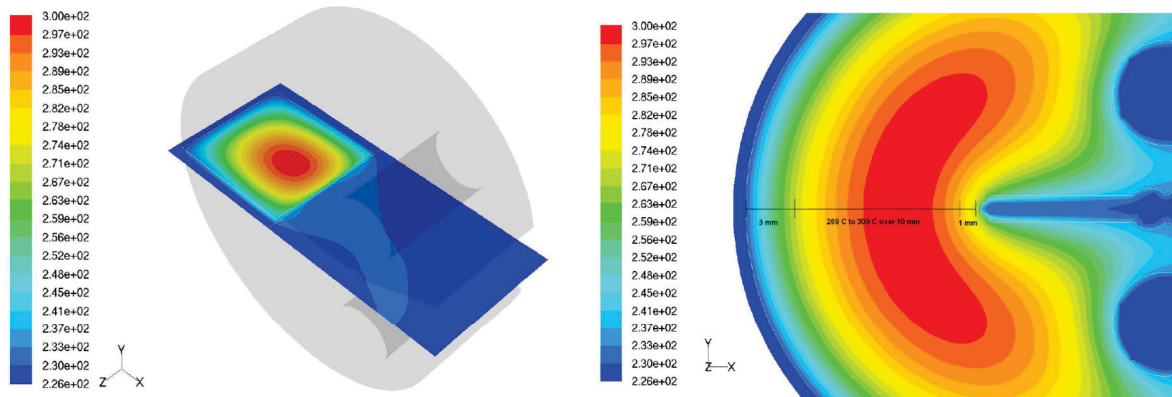


Figure 5. Temperature gradient obtained for a 0.5-CT specimen at the maximum flux rate considered in this report.(Tyler 2014)

1.3 Data Required

Data are needed to quantify the effectiveness of HWC mitigation on CGR for material at fluence above $3 \times 10^{21} \text{ n/cm}^2$ (4 dpa) as a function of K applied. Based on the estimated fluence to be experienced by the component, operational K (discounting any relaxation effect), and previous data, it is recommended that CGR data be generated in the NWC and HWC environments under K applied, ranging from 14 to 22 ksi $\sqrt{\text{in}}$ from specimens of accumulated fluence above $3 \times 10^{21} \text{ n/cm}^2$ (4 dpa) and up to $7 \times 10^{21} \text{ n/cm}^2$ (10 dpa). Ideally, the total fluence should be accumulated in a spectrum and flux rate comparable to a BWR (such as permitting direct transposition of data to components in service). However, a higher flux rate would be acceptable when justified by previous experiences and the known impact of flux rate on irradiated microstructure. The materials will need to be 300-series austenitic stainless steels (Type 304, 304L, 316L, 316NG, or 304NG), their welds, and heat affected zone (HAZ) (304HAZ and 316 HAZ). Typically, each material should be tested under several K alternatively in NWC and HWC at a given dose. Ideally, each material would be available at different dose levels.

CGR data are needed to determine the effect of fluence on the efficiency of HWC mitigation. However, it would be a mistake to only consider the short-term and immediate need for such data. The prediction of CGR and development of predictive models that will be able to predict SCC often requires a different set of data. This is why, in this report a quick description of techniques used to study the fundamentals of SCC is proposed and why it will be suggested that, when possible, material be harvested or generate in addition to the specimen immediately needed for this program. These additional materials and specimens could be made available to the scientific community through the U.S. Department of Energy Advanced Test Reactor's National Scientific User Facility for future research projects. These projects would benefit a direct comparison with the CGR data to be generated by this program.

It would be beneficial to move from an empirical estimation of specimen K-size validity to a model more based on actual material mechanical response.

Fracture toughness data above $3 \times 10^{21} \text{ n/cm}^2$ (4 dpa) also are desirable in order to define a transition to lower fracture toughness at fluences above $3 \times 10^{21} \text{ n/cm}^2$ (4 dpa). Although fracture toughness is not the topic of this report, it will be recommended that fracture toughness testing be performed after CGR testing when possible.

2. PROGRAM PLANS

Three program plans and their options are discussed in this report. Although they do not exclude each other, they are presented separately based on the origin of the material tested and on the equipment requirements. The facilities available to perform neutron irradiation with the specimen size required for

this program and to perform IASCC experiments are limited. Therefore, several options will be presented that can be chosen from, based on the funding and equipment availability. A summary section will summarize these programs, discuss how they can overlap, and discuss how they can feed future programs.

2.1 Program Plan Based on an Irradiation Program Dedicated to this Work

A dedicated irradiation and test program can be defined to generate the required CGR data. This irradiation program has the benefit of circumventing heat-to-heat variability by testing the heat of each material over the range of fluence and determined applied K. It also would permit generation of specimens, whose size will not limit testing due to a K size validity criterion.

This program proposes to generate specimens to quantify the efficiency of HWC under applied K, ranging from 14 to 22 ksi $\sqrt{\text{in}}$ to doses ranging from 2 to 10 dpa. Three dose levels between 4 and 10 dpa are desirable. Data at 2 dpa would permit tying the new data to the various data available and would serve as a baseline, because HWC mitigation is expected to be efficient at such a dose under the commonly applied K. Following the irradiation program, microstructure and mechanical properties will be characterized. A CGR testing plan will be discussed.

In this report, the specimen design, cost estimate, and schedule have been determined based on the assumption that irradiation will be performed in the water loop located in the Advanced Test Reactor center flux trap (ATR 2009).

2.1.1 Material Selection

The materials of interest are stainless steels and their welds. For this program, it was decided to focus on four materials to minimize the size of the irradiation matrix. Two base metals (304L and 316L) and their weld HAZ were selected. The materials will be welded under constrained conditions using shielding metal arc welding in conditions consistent with those typical of BWR core components.

Complete traceability of the material will be required. The material will be procured in enough quantity to have sufficient archive material to support other future irradiation programs.

2.1.2 Specimen Design

2.1.2.1 T-CT Specimen. Various geometries were considered as to be able to test in the large K range considered. Based on the estimation presented in Tables 1 and 2, a program involving 316L material could be performed with 0.4 T-CT specimens for a dose of about 2 dpa, and 0.4 T-CT specimens with 0.3-in. thickness can be used for higher doses. The mechanical properties predicted for irradiated 304 stainless steel call for use of 0.6 T-CT specimens for irradiation around 2 dpa; 0.4 T-CT specimens will be used for irradiation up to around 4 dpa; and 0.4 T-CT with 0.3-in. thickness will be used for specimens to be irradiated at higher doses.

The specimens made of base metal will be cut in the T-S orientation from a plate. A 5% side groove will be machined. The schematic of a 0.4 T-CT specimen is presented in Figure 6. For HAZ specimens, the CT specimens will be cut so the crack grows in the HAZ.

2.1.2.2 Tensile and TEM Specimen. Tensile and TEM specimens will be included in the irradiation for each target dose. The TEM specimens will consist of 3-mm disks. The tensile specimens will be dog bone specimens similar to the one shown in Figure 7.

2.1.3 Irradiation and Test Plan

2.1.3.1 Selection of Dose Rate and Temperature. The dose rate in a BWR is about 2×10^{13} n/cm²-sec. Under such a low flux rate, it would not be possible to generate specimens with the dose range required in a timely manner. Significantly increasing the dose rate experienced by the specimen raises the question of the flux rate's effect on the material microstructure and the CGR

behavior. This flux rate effect has been demonstrated at low dose. However, it appears that in the region of 3 to 5 dpa, the flux rate effect is negligible on the factors influencing CGR (Radiation Induced Segregation, hardening). Therefore, it is considered to be target dose rates similar to the ones used for a similar program at the Japanese Material Test Reactor (JMTR) (1×10^{14} n/cm^{2-s} or about 2×10^{-7} dpa/s). The Advanced Test Reactor's center flux trap offers about 2×10^{-7} dpa/s (ATR 2009). An irradiation in this position would permit generation of specimens with up to 10.5 dpa within 4 years. The data would be directly comparable with the data generated by the Japanese program with specimens irradiated in JMTR. It is therefore proposed to perform the irradiation program at the ATR. However, considering that a lower flux would be technically acceptable, other reactors can be considered although the period of irradiation will be extended.

The target irradiation temperature will be 288°C.

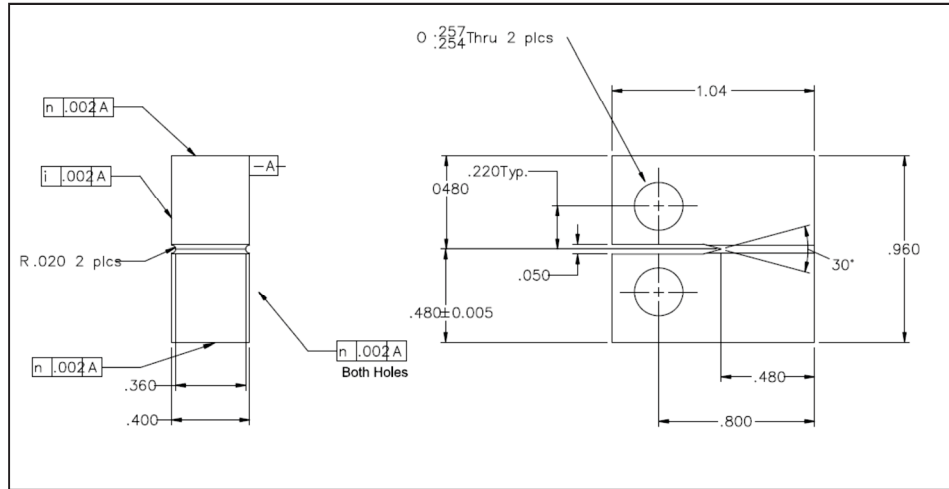


Figure 6. Schematic of the 0.4 T-CT specimen dimensions in inches.

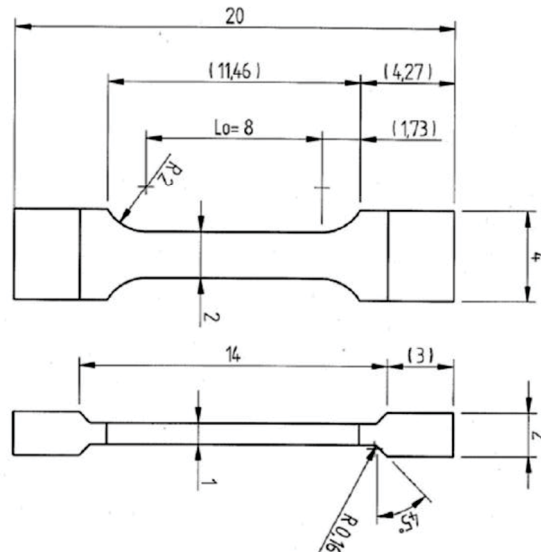


Figure 7. Schematic of a tensile specimen dimension in inches.

2.1.4 Test Plan and Outcome

The irradiation is designed to use about two-thirds of the more valuable real estate of the Advanced Test Reactor in order to increase the availability of the irradiation position. The target doses for the specimens are 2.5, 4.3, 7.7, and 10.3 dpa. The specimen's size will differ as a function of final dose in order to meet the K-size criteria previously determined (Tables 3 and 4). For 316-type stainless steel, the 0.4 T-CT specimen will be used for the target dose of 2.5 dpa and the 0.4 T-CT specimen with a thickness of 0.3 in. will be used for higher doses. For 304-type stainless steel, the 0.6 T-CT specimen will be used for a target dose of 2.5 dpa, the 0.4 T-CT specimen will be used for the target dose of 4.3 dpa, and the 0.4 T-CT specimen with a thickness of 0.3 in. will be used for higher doses. The test train is composed of four test capsules. Three test capsules will be located in the core of the reactor and will experience a dose rate of 1.5×10^{-2} dpa/day. A fourth capsule will be located about 9 in. from the center of the core and the dose rate will be about 0.7×10^{-2} dpa/day. The purpose of the different locations is to minimize temperature gradient through specimens of different thicknesses. Each capsule will contain CT specimens, tensile specimens, and TEM discs for one target dose. The target dose for each capsule is indicated in Table 3. Capsule D will contain four 0.6 T-CT specimens of 304L and 304HAZ. Capsule A and B, for target doses of 10.26 and 7.69 dpa, respectively, will contain thin 0.4 T-CT specimens of 304L, 304LHAZ, 316L, and 316LHAZ. Capsule C, for a target dose of 4.28 dpa, will contain 0.4 T-CT specimens of 304L and 304LHAZ, and thin 0.4 T-CT specimens of 316L and 316LHAZ. When Capsule B is removed after the specimens reach 7.69 dpa, the specimens will be replaced by 0.4 T-CT specimens of 316L and 316LHAZ. This irradiation plan will generate the minimum number of specimens required in 3 years.

Table 3. Target dose for the irradiation program. The value in bold corresponds to the dose at which a capsule is removed and specimens are made available.

Capsule		A	B	C	D
Year	Cycle	Dose (dpa)	Dose (dpa)	Dose (dpa)	Dose (dpa)
1	1	0.85	0.85	0.85	0.5
	2	1.71	1.71	1.71	1
	3	2.56	2.56	2.56	1.5
	4	3.42	3.42	3.42	2
2	5	4.28	4.28	4.28	2.5
	6	5.13	5.13		
	7	5.985	5.985		
	8	6.84	6.84		
3	9	7.69	7.69		
	10	8.55	0.85		
	11	9.40	1.71		
	12	10.26	2.56		

After exposure, each specimen will be tested. Tensile specimens will be used to determine the mechanical properties of the material at the achieved dose. TEM discs will be used for microstructure analysis. The CGR specimens of the four heats of materials will be tested at K, ranging between 14 ksi $\sqrt{\text{in}}$ (15.4 Mpa $\sqrt{\text{m}}$) and 22 ksi $\sqrt{\text{in}}$ (24.2 Mpa $\sqrt{\text{m}}$). The details of the test procedure are provided in Appendix A. An example of the test plan for alloy 316L is presented Table 4. The maximum target K was selected to be conservative; knowing that uncertainty in crack length measurement by dcPd may lead to an underestimation of K and sometime threaten the validity of the test. It is always the responsibility of

the experimenter to estimate the validity of the CGR measured and determine if applying higher K and extending the initial K range can be done.

Table 4. Test plan for 316L specimens.

Material	316L											
Dose (dpa)	2.56			4.28			7.69			10.26		
Number of specimen	3			3			3			3		
K tested (ksi√in)	14			14			14			14		
		16			16			16			16	
	18			18			18			18		
		20			20			20			20	
			22			22			22			22
Fracture toughness			yes			yes			yes			yes
Environment per K tested	NWC and HWC											

This program will generate CGR versus K curves for four levels of fluences and quantify the effectiveness of HWC for materials experiencing up to 80 years of service.

2.1.5 Estimate Cost

The timeline and cost for the irradiation activity is presented in Table 5. Once the target dose is achieved for a capsule, the mechanical properties and microstructure of the materials containing a capsule can be characterized in the year following removal of this capsule from the reactor. For each material-dose couple, three CGR tests will be performed, which is about 1 year of occupancy of a CGR test loop. The plan calls for four materials and four doses, which is about 16 years of occupancy of a test loop to test all specimens and complete the test plan. A detailed timeline to complete the test plan is not provided because it is obvious that the availability of test loops in the country for the next 16 years is not available. This project would benefit from collaboration between laboratories to obtain data in a timely manner.

Table 5. Estimated timeline and associated cost for the irradiation program.

	Activity (Irradiation Related) and Specimens Available For Testing	Estimated Cost (\$K)
Year 1	Design, fabrication of test train and specimens Irradiation test plan	1,200
Year 2	Ongoing Capsule A, B, C, and D	700
Year 3	Ongoing Capsule A and B 304 materials at 2.5 dpa available All materials at 4.28 dpa available	720
Year 4	All materials at 7.69 and 10.26 dpa available 316 materials at 2.56 dpa available	740

2.2 Program Based on Material Harvested from Boiling Water Reactor Components

The primary objective of this program is to determine the validity of the disposition curve at fluences above 3 dpa by determining the evolution of CGR as K increases for material harvested from BWR

components. The use of such material assures that the material is fully representative of what is in the field, but it also limits the range of fluence available. However, it is possible to extend the range of fluence available with a dose accumulation program. This program is described as an additional test plan and designed based on the considerations discussed in the previous section.

2.2.1 Material and Specimens

Collaboration with General Electric would permit gaining access to materials removed from the cruciform region of five control rod blade handles. The materials, three heats of 316NG and two heats of 304NG, experienced up to 3.8×10^{21} n/cm² (5.4 dpa) in service. Mechanical characterization and microstructure analysis are available for these materials. The accumulated fluence was estimated using the power history of the reactor and was compared to retrospective dosimetry. The materials composition and accumulated fluence are presented in Table 6. The material currently is present in the United States and could be made available for this research program. More information concerning these materials is available in Appendix B.

Table 6. Control rod blade material available through collaboration.

Heat ID	Material type	Dose ($\times 10^{21}$ n/cm ²)	Dose (dpa)
D802	316NG	2.8	4
D800	316NG	1.2	1.7
D790	316NG	2.1	3
D485	304NG	3.8	5.42
SND482	304NG	3.2	4.57

Due to the thickness of the source material, the specimen will be based on a standard 0.4 T-CT specimen, but with a thickness of 0.3 in. The maximum allowable K for each material type is determined using Table 2. These no-standard-specimens should offer sufficient ligaments for crack grow for the various tests segments needed for the project.

2.2.2 Test Plan and Outcome

Initially, testing of two heats of 316 stainless steel and two heats of 314 stainless steel is proposed. Part of this set of material had been tested previously and data had been reported by Horn et al. (2013). The data showed that HWC was effective when alloy D482 (i.e., a type 304NG stainless steel at 4.5 dpa) was tested at an applied K of 15 ksi√in (16.5 Mpa√m). HWC mitigation was not effective for two heats of Type 316NG stainless steel (i.e., D790 tested under K greater than 23 ksi√in [25.3 Mpa√m] and D790 tested under K greater than 18.7 ksi√in [20.5 Mpa√m]), although doses were slightly lower (4 dpa for D802 and 3 dpa for D790). Such data needs to be extended to be able to quantify the efficiency of HWC in a broader range of K applied for each heat. The heat of 304NG stainless steel (SND485), which experienced 5.4 dpa in service, will be added to this work scope. The objective will be to determine the validity of the CGR disposition curves for fluence above 2.1×10^{21} n/cm² (3 dpa) and below 3.8×10^{21} n/cm² (5.4 dpa).

The four heats of material will be tested at K ranging between 14 ksi√in (15.4 Mpa√m) and 22 ksi√in (24.2 Mpa√m) for 316 and between 14 ksi√in (15.4 Mpa√m) and 20 ksi√in (22 Mpa√m) for 304. These data would permit determination of the validity of the CGR disposition curve in the HWC condition at the fluence tested, determine if the current disposition curves are conservative for a given K, and provide information to determine if the industry can take credit for stress relaxation. The summary of the tests is presented in Table 7.

Table 7. Test plan for materials issued from harvested components.

Specimen ID	D802			D790			D485		D482	
Material	316NG			316NG			304NG		304NG	
Dose (dpa)	4			3			5.4		4.5	
Number of Specimen	3			3			2		2	
K Tested (ksi√in)	14			14			14		14	
		16			16			16		16
	18			18			18		18	
		20			20			20		20
			22			22				
Fracture Toughness?			yes			yes		yes		yes
Environment per K Tested	NWC and HWC									

2.2.3 Estimated Timeline and Cost

Table 8 presents the estimated timeline and cost to perform the work described in this section, assuming the CGR work is performed at Idaho National Laboratory. This estimate does not consider equipment availability and assume that one IASCC test loop will be available for this program when needed. This work represents a 6-year-long effort for a cost (excluding shipping) of about \$1,300K over this period.

Table 8. Estimated timeline and cost assuming that the work is performed at Idaho National Laboratory for the basic test plan.

	Activity	Outcome	Estimated Cost (\$K)
Year 1	Material shipment Specimen machining	Material available for testing.	200
Year 2	Testing heats D802 and D790: two tests		280
Year 3	Testing heats D802 and D790 continued: two tests	Quantification of the efficiency of HWC mitigation for two heats of 316NG as a function of K applied (ranging from 14 to 20 ksi√in) at fluence above 3.2×10^{21} n/cm ² (4.5 dpa).	280
Year 4	Testing heats D482 and D485: two tests		280
Year 5	Testing heats D482 and D485 continued: two tests	Quantification of the efficiency of HWC mitigation for two heats of 304NG as a function of K applied (ranging from 14 to 20 ksi√in) at fluence above 2.1×10^{21} n/cm ² (3 dpa). Fracture toughness data.	280
Year 6	Testing heats D802 and D790 continued: two tests	Quantification of the efficiency of HWC mitigation for two heats of 316NG at K applied (about 22 ksi√in) at fluence above 3.2×10^{21} n/cm ² (4.5 dpa). Fracture toughness.	280

2.2.4 Additional Irradiation Program and Test Plan

It would be desirable to establish the evolution of CGR for a given K as fluence increases. Attaining this objective will require irradiating specimens up and beyond 5 dpa. Using the heat D800 (316NG material) is proposed, which experienced 1.2×10^{21} n/cm² (1.7 dpa), in service and to re-irradiate this material to have four accumulated fluences ranging from 1.2×10^{21} n/cm² (1.7 dpa) to 6×10^{21} n/cm² (8.5 dpa). This irradiation could be performed as a stand-alone irradiation or be part of the irradiation program described previously. The material will be tested in both NWC and HWC under five applied K, with K ranging between 14 ksi√in (15.4 Mpa√m) and 22 ksi√in (24.2 Mpa√m). For each irradiation condition, the mechanical properties and microstructure analysis will be performed. An estimated timetable for this activity is presented in Table 9. In accordance with the irradiation condition, this work would require three CT specimens, two tensile specimens, and TEM discs.

This additional work will provide CGR data with the same material as a function of fluence and applied K. It will provide insight about the validity of high-flux rate irradiation in this dose range.

Table 9. Estimated timetable for additional activity with control rod blade material.

Year	Dose Available	Activity
0	1.7	CGR at 1.7 dpa K = 14 to 20 ksi√in
1	4	CGR at 4 dpa K = 14 to 22 ksi√in Comparison with D802 results (4 dpa accumulated in reactor)
2	7	CGR at 7 dpa K = 14 to 22 ksi√in
3	10	CGR at 10 dpa K = 14 to 22 ksi√in

2.3 Programs Based on Materials Generated by a Previous Irradiation Program

The objective of the primary program of this section is to determine the evolution of CGR as a function of applied K on a single heat of material for three fluence levels. Working with a single heat of material permits prevention of data scatter due to heat-to-heat variability and will clearly show the influence of fluence in the CGR behavior of the material. Moreover, the material selected represents the fusion zone of a 304L weld and few data are available for welds.

The suggested extended program is similar to the work proposed with material harvested from BWR components where it will determine the evolution of CGR as a function of K applied at a given fluence. Additional interest resides in the testing of HAZ (304L and 316L). No HAZ was available from harvested components and HAZ is of interest, and of HT 304L with a dose greater than 10 dpa, which corresponds to the maximum dose to be experienced by components after 80 years of life extension.

2.3.1 Materials and Specimens

The materials come from a Japanese national project that started in 2001. Specimens were irradiated in JMTR in BWR conditions (e.g., temperature of 288°C [262 to 302°C] and conductivity below 0.1μS/cm [Takakura et al. 2009, Nakamura et al. 2007) at a flux rate of 1×10^{18} n/m^{2-s}). Some post-irradiation experiments (e.g., mechanical testing, microstructure characterization and CGR) have been performed and the data are available. For this project, heat-treated 304 (SUS 304HT), heat treated 316L (316LHT), and HAZ (304L and 316L) were selected. The heat treatment applied (i.e., 1030°C for 30 minutes, followed by water quench) diminished the enriched chromium (and molybdenum) concentration at grain boundaries of the as-received materials to simulate the new fusion line of the weld HAZ. The HAZ specimens were generated from the plate of 316L and 304L welded using shielded metal arc welding under conditions typical for most BWR core components. The D316L electrode was used to

weld 316L and D308L was used to weld 304L. The specimens selected for the programs discussed in this report are presented in Table 10 (primary program) and Table 11 (extended program).

The specimens' designs are based on a standard 0.5 T-CT specimen design, but with varied thicknesses (e.g., for a specimen with less than 1.7 dpa and specimen thickness of 0.5 in. [12.7 mm] and for specimens with up to 5 dpa and specimen thickness of 0.25 in. [6.4 mm]). For specimens with higher doses, the specimen thickness is 0.22 in. (5.6 mm). The specimens were cut in the T-S orientation. Assuming an irradiation hardening similar to that discussed earlier in this report (Demma 2010), and using ASTM Standard E399 and E647 as references with a discount factor of two, specimens A105 and A106 can be tested up to $K = 20.7 \text{ ksi}\sqrt{\text{in}}$ (22.8 $\text{Mpa}\sqrt{\text{m}}$) and grow the crack with little constraint ($a/w = 0.6$ can be safely achieved). Specimens A128 and A129 can be tested up to $K = 21.8 \text{ ksi}\sqrt{\text{in}}$ (24.0 $\text{Mpa}\sqrt{\text{m}}$).

Table 10. Specimens available for the main program.

Specimen ID	A105	A106	A128	A129	A139	A140
Material	304HT				304LHT	
Dose (dpa)	3.82	4.49	8.6	8.9	13.6	13.4

Table 11. Specimens available for the extended program.

Specimen ID	A112	A113	A114	A102	A104
Material	304L/HAZ			304/HAZ	316L/HAZ
Dose (dpa)	3.81	3.57	3.75	3.29	3.72

2.3.2 Test Plan and Outcome

Four specimens made of 304HT and two made of 304LHT will be tested successively in NWC and HWC at $K = 14, 16, 18,$ and $20 \text{ ksi}\sqrt{\text{in}}$. The doses experienced by the selected specimens are roughly 4 dpa, 8.5 dpa, and 13.5 dpa. This range will permit demonstration of the effect of fluence on the CGR dependency to applied K . The test plan suggests testing only two K per specimen. For each K applied, two water chemistries (i.e., NWC and HWC) are to be tested. The test conditions and procedure are described in Appendix A. Table 12 presents the test plan suggested for this program.

Table 12. Stress intensity factor applied to HT304 specimens for the primary program.

Specimen ID	A105	A106	A128	A129	A139	A140
Dose (dpa)	3.82	4.49	8.6	8.9	13.6	13.4
K tested ($\text{ksi}\sqrt{\text{in}}$)	14		14		14	
		16		16		16
	18		18		18	
		20		20		20
Fracture toughness?		yes		yes		yes
Environment per K tested	NWC and HWC					

2.3.3 Estimated Timeline and Cost

This program will need shipping of specimens from Japan to the United States. This estimate assumes that the work will be performed at Idaho National Laboratory and that no collaboration is established with the current owner of the specimens (located in Japan). Equipment availability is not considered. The cost

and timeline associated with this activity is presented in Table 13. The work represents a 4-year-long effort for a cost (excluding specimen acquisition and shipping) of about \$850K over this period.

Table 13. Estimated timeline and cost for the primary program using specimen generated from a previous irradiation program.

	Activity	Outcome	Estimated Cost (\$K)
Year 1	Specimen acquisition, shipment and reception	Material available for testing in the United States.	?
Year 2	Testing specimens A128 and A129		280
Year 3	Testing specimens A105 and A106	Determination of the influence of fluence on the evolution of CGR for 304HT as a function of K. Fracture toughness data.	280
Year 4	Testing specimens A139 and A140	Determination of the influence of K applied on the evolution of CGR for 304L at fluence corresponding to the end of component lifetime. Connection, although with reserve, with 304HT data at lower dose . Fracture toughness data.	280

2.3.4 Extended Program

The CGR of 304L HAZ, 304HAZ and 316L HAZ at around 4 dpa will be measured at four applied K ranging from 14 to 20 ksi $\sqrt{\text{in}}$. These data will permit comparison of HAZ behavior with base metal and the applicability of the disposition curve to the welds. Table 14 presents the test plan suggested for this program. As only one specimen is available for 304HAZ and 316L HAZ, it is expected that the results obtained with 304L HAZ will allow planning the future experiments to select the K applied accordingly. In addition, fracture toughness data will be generated, assuming satisfactory behavior of the crack.

Table 14. Test plan for the extended program.

Specimen ID	A112	A114	A102	A104
Material	304L HAZ		304 HAZ	316L HAZ
Dose (dpa)	3.81	3.75	3.29	3.72
K Tested (ksi $\sqrt{\text{in}}$)	14		14	14
		16		
	18		18	18
		20		
Fracture Toughness?		yes		
Environment per K Tested		NWC and HWC		

The cost and timeline associated with this activity are presented in Table 15. This work represents a 5-year-long effort for a cost (excluding specimen acquisition and shipping) of about \$1100K over this period.

Table 15. Estimated timeline and cost associated with the extended program.

	Activity	Outcome	Estimated Cost (\$K)
Year 1	Specimen acquisition, shipment and reception	Material available for testing in the United States.	?
Year 2	Testing specimens A112 and A114	Determination of the evolution of CGR as a function of K for 304L HAZ at about 4 dpa. Fracture toughness data.	280
Year 3	Testing specimens A115 and A116	Determination of the evolution of CGR as a function of K for 316L HAZ at about 4 dpa. Fracture toughness data.	280
Year 4	Testing specimens A130 and A131	Determination of the evolution of CGR as a function of K for 316L HAZ at about 10 dpa. Fracture toughness data.	280
Year 5	Testing heats A127 and A138	Determination of the evolution of CGR as a function of K for 316L HAZ at about 13 dpa. Fracture toughness data.	280

3. COLLABORATIONS AND BENEFIT TO OTHER FUNDAMENTAL PROGRAMS

In this report, three test plans, often with an associated extended plan, were presented. Each test plan came with a significant need of resources, both in funding requirement and test equipment. It should be noted that parts of these plans could be performed simultaneously without much cost increase. For instance, the irradiation program proposed as an extended program with the materials harvested from BWR components could be merged with the main irradiation program at low cost. The work proposed with materials previously irradiated at JMTR can lead to collaboration with the owners of the materials, which would allow the program to free U.S. facilities for other parts of the proposed program and generate data faster. All test plans call for long experiments. In addition, over 20 years of test loop usage will be necessary. It would be in the interest of this program to take advantage of any facility available to coordinate the testing (such as obtaining data in timely fashion). International support could be appropriate and may be a requirement when the program plan requires usage of specimens owned by a foreign entity. In this particular case, collaboration would forfeit any cost associated with the acquisition of the specimens.

This report focuses on determining the efficiency of HWC mitigation as fluence increases by generating CGR data. However, the fundamental reason for a change in HWC efficiency should be explored, because such work is likely to increase our understanding of the IASCC mechanism. It was suggested that the changes in local deformation play a significant role in CGR and that local deformation should be taken into account to develop a CGR model for highly irradiated steels. To be able to determine the correlation between CGR and local deformation, it would be beneficial to perform specific local deformation experiments with the same material used for CGR characterization. Similarly, programs investigating the behaviors of such materials (Stephenson and Was 2014, Gussev et al. 2013, and Gussev et al. 2014) would gain by having access to the materials this program will generate. Considering the effort and funds invested in accessing and generating such materials, collaboration with the Advanced Test Reactor's National Scientific User Facility is suggested to reach out to various U.S. Department of

Energy-funded researchers to determine the potential use of additional specimens to be generated before starting an irradiation program or acquisition and shipment of irradiated materials. The specimens generated could be managed by the Advanced Test Reactor's National Scientific User Facility, offered to users via the sample library under the condition that the work performed benefits this program and other U.S. Department of Energy Office of Nuclear Energy programs.

4. REFERENCES

- Andresen, P. L., T. M. Angeliu, L. M. Young, W. R. Catlin, and R. M. Horn, 2002, *10th International Conference on Environmental Degradation of Materials in Nuclear Power Systems— Water Reactors*.
- Andresen, P. L. and M. M. Morra, 2008, *Journal of Nuclear Materials*, Vol. 383 (1-2).
- Andresen, P. L., 2011, "K Size Effects on SCC in Irradiated, Cold Worked and Unirradiated Stainless Steel," *11th International Conference on Environmental Degradation of Materials in Nuclear Power Systems – Water Reactors*.
- ASTM E 399, "Standard Test Method for Linear-Elastic Plane-Strain Fracture Toughness K_{Ic} of Metallic Materials," American Society of Testing and Materials.
- ATR, "Advanced Test Reactor National Scientific Users' Guide", INL Report Number INL/EXT-08-14709, 2009.
- Demma, A., 2010, MRP-135, Revision 1, Electric Power Research Institute.
- Gushev, M. N., J. T. Busby, T. S. Byun, and C. M. Parish, 2013, "Twinning and martensitic transformations in nickel-enriched 304," *Materials Science and Engineering A*, Vol. 588, pp. 299–307.
- Gushev, M. N., K. G. Field, and J. T. Busby, 2014, "Strain-induced phase transformation at the surface of an AISI-304," *Journal of Nuclear Materials*, Vol. 444, pp. 187–192.
- Hazelton, W. S. and W. H. Koo, 1988, NUREG-0313, Revision 2, U.S. Nuclear Regulatory Commission.
- Horn, R. M., R. Hosler, P. Chou, and P. L. Andresen, 2013, "Studies of Crack Growth Rates in Irradiated Stainless Steel Control Blade Materials Tested in High Temperature Water," *16th Intl. Conf. on Environmental Degradation of Materials in Nuclear Power Systems – Water Reactors*, Asheville, NC.
- Jensen, A., K. Gott, P. Efsing, and P. Anderson, 2003, "Crack Growth Behavior of Irradiated Type 304L Stainless Steel in Simulated BWR Environment," *11th Intl. Conf. on Environmental Degradation of Materials in Nuclear Power Systems – Water Reactors*.
- Jensen, A. J. Stjarnsater, and R. Pathania, 2009, "Crack Growth Rate Testing of Fast Reactor Irradiated Type 304L and 316 SS in BWR and PWR Environments," *14th Int. Conf. on Environmental Degradation of Materials in Nuclear Power Systems*, Virginia Beach, VA.
- Nakamura, T., M. Koshiishi, T. Torimaru, Y. Kitsunai, K. Takamura, K. Nakata, M. Ando, Y. Ishiyama and A. Jensen, 2007, "Correlation between IASCC Growth Behavior and Plastic Zone Size of Crack Tip in 3.5 Neutron Irradiated Type 304L SS CT Specimen," *13th International Conference on Environmental Degradation of Materials in Nuclear Power Systems – Water Reactors*, Whistler, British Columbia.
- Pathania, R., R. Carter, R. Horn, and P. Andresen, 2009, "Crack Growth Rates in Irradiated Stainless Steels in BWR Internals," *14th Intl. Conf. on Environmental Degradation of Materials in Nuclear Power Systems – Water Reactors*.
- Stephenson, K. J. and G. S. Was, 2014, "Crack initiation behavior of neutron-irradiated model and commercial," *Journal of Nuclear Materials*, Vol. 444, pp. 331–341.

- Sumiya, R., S. Tanaka, K. Nakata, K. Takakura, M. Ando, T. Torimaru, and Y. Kitsunai, 2007, “K Validity Criterion of Neutron Irradiated Type 316L Stainless Steel CT Specimen for SCC Growth Test,” *13th International Conference on Environmental Degradation of Materials in Nuclear Power Systems*, Whistler, British Columbia.
- Takakura, K., K. Nakata, S. Tanaka, T. Nakamura, K. Chatani, and Y. Kaji, 2009, “Crack Growth Behavior of Neutron Irradiated L-Grade Austenitic Stainless Steels in Simulated BWR Conditions,” *14th Intl. Conf. on Environmental Degradation of Materials in Nuclear Power Systems – Water Reactors*, Virginia Beach, VA.
- Tyler, C.R.; Murray, P.E.; Nielsen, J.W., "CRADA EPRI Phase II Design Report, Revision 1", INL Report Number INL/LTD-12-24400, February, 2014.

Appendix A

CGR Test Procedure

CGR testing will be performed in simulated BWR primary water on the CT specimens provided. The test will be connected to a water loop operating under representative BWR operative conditions. The loop will operate at 288°C (550°F) and a pressure of about 10 MPa (1,450 psi). The effluent water conductivity will be maintained below 0.1 µS/cm. For testing in NWC, the dissolved oxygen content will be about 2 ppm, and for testing in HWC, the low potential environment will be obtained by maintaining about 100 ppb of hydrogen in the water. The test system will be equipped with a dcpd monitoring technique to follow crack advance and control applied K.

The specimen will be loaded into the autoclave and test conditions (i.e., pressure, temperature, and water chemistry) will be stabilized. A starter fatigue crack will be developed in the CT specimen, followed by transitioning of the fatigue pre-crack to a SCC. Following fatigue pre-cracking and SCC transitioning (Steps 1 through 6 in Table A-1), testing shall continue under constant stress intensity to measure the CGR at two stress intensity levels, alternatively in NWC and HWC. Depending on the CGR response, steps with gentle fatigue (i.e., partial periodic unloading with a hold time at a maximum load for 9,000 seconds) may be introduced during the course of the test. The stress intensity should be progressively increased using dK/da (Step 11). The duration for each step is indicative. It is expected that the experimenter will adjust the duration of the test under a given set of condition based on the response of CGR. In the environments and loading considered, CGR should be somewhere between 7×10^{-10} mm/s and 7×10^{-6} mm/s. Under such CGR, a crack increment of 0.1 mm will take between 4 and 40,000 hours. Therefore, it is obvious that the duration of each step will be related to the CGR obtained.

Furthermore, depending on the crack growth response of the specimens, appropriate adjustments to the test sequence may be required. This could involve introduction of steps for SCC transitioning where the frequency and/or R value are changed in smaller increments than shown in Table A-1. The exact length of the test will be dictated by the response of the sample. Continuous digital records of all relevant data will be kept throughout the entire test of each specimen.

Subsequent to testing, all specimens shall be broken open to determine the actual crack length. In addition, all specimens shall be subjected to fractographic examination by scanning electron microscopy.

It is intended that fracture toughness testing be performed on specimens used in CGR testing if sufficient ligament remains in these specimens.

Table A-1. Example of test procedure.

Steps	K	R	F	Environment	Crack Increment mm	Final a/w
1	13	0.2	1	NWC	1	0.44
2	14	0.6	1	NWC	0.1	0.444
3	14	0.6	0.1		0.1	0.448
4	14	0.6	0.01		0.1	0.450
5	14	0.6	0.001		0.1	0.456
6	14	0.6	0.001+hold		0.1	0.460
7	14	1	constant	NWC	0.4	0.476
8	14	1		HWC	0.2	0.484
9	14	1		NWC	0.4	0.5
10	14	1		HWC	0.2	0.508

Steps	K	R	F	Environment	Crack Increment mm	Final a/w
11	14	1		NWC	0.2	0.516
12	14 to 18		dK/da	NWC	0.4	0.532
13	18	1		NWC	0.4	0.548
14	18	1		HWC	0.4	0.564
15	18	1		NWC	0.2	0.572
16	18	1		HWC	0.2	0.58

Appendix B

Data Concerning Control Rod Blade Materials Available

Table 2-2. Compositions for Each Control Blade (From GE-VNC)

Blade	C	Mn	P	S	Si	Ni	Cr	Mo	Co	Cu	N
D802	0.011	1.71	0.014	0.005	0.46	10.43	16.48	2.10	0.03	0.07	0.090
D800	0.011	1.71	0.014	0.005	0.46	10.43	16.48	2.10	0.03	0.07	0.090
D790	0.011	1.71	0.014	0.005	0.46	10.43	16.48	2.10	0.03	0.07	0.090
D485	0.017	1.71	0.018	0.018	0.39	9.33	18.47	0.05	0.03	0.06	0.082
D482	0.017	1.71	0.018	0.018	0.390	9.33	18.47	0.05	0.03	0.060	0.082
Fe60R	0.08	1.46	0.026	0.029	0.49	8.51	19.04	-	-	-	-

*Fe is the balance on all samples

Table 2-1. Irradiation History Summary
(All TaiPwr samples were removed from the reactor on
March 31, 2001, but inserted at different times)

Sample	Reactor Source	Cycles	# 6-Week Insertions	Total Days	EFPD**	Projected Dose (x 10 ²¹ n/cm ²)
D802 (316NG)	TaiPwr	11-14	10	1977	449.91	2.8
D800 (316NG)	TaiPwr	11-14	2	1043	126.57	1.2
D790 (316NG)	TaiPwr	11-14	9	1977	383.08	2.1
D485 (304NG)	TaiPwr	9-14	15	2905	656.24	3.8
SND482 (304NG)	TaiPwr	9-14	10	2905	481.01	3.2
Fe-60R (304SS)	Millstone	*	*	*	*	*

* - Unknown ** - Effective Full Power Days